JCI The Journal of Clinical Investigation

Cigarette smoke selectively enhances viral PAMP– and virus-induced pulmonary innate immune and remodeling responses in mice

Min-Jong Kang, … , Richard Enelow, Jack A. Elias

J Clin Invest. 2008;118(8):2771-2784. https://doi.org/10.1172/JCI32709.

Research Article

Viral infections have more severe consequences in patients who have been exposed to cigarette smoke (CS) than in those not exposed to CS. For example, in chronic obstructive pulmonary disease (COPD), viruses cause more severe disease exacerbation, heightened inflammation, and accelerated loss of lung function compared with other causes of disease exacerbation. Symptomatology and mortality in influenza-infected smokers is also enhanced. To test the hypothesis that these outcomes are caused by CS-induced alterations in innate immunity, we defined the effects of CS on pathogen-associated molecular pattern–induced (PAMP-induced) pulmonary inflammation and remodeling in mice. CS was found to enhance parenchymal and airway inflammation and apoptosis induced by the viral PAMP poly(I:C). CS and poly(I:C) also induced accelerated emphysema and airway fibrosis. The effects of a combination of CS and poly(I:C) were associated with early induction of type I IFN and IL-18, later induction of IL-12/IL-23 p40 and IFN-γ, and the activation of double-stranded RNA-dependent protein kinase (PKR) and eukaryotic initiation factor-2α (eIF2α). Further analysis using mice lacking specific proteins indicated a role for TLR3-dependent and -independent pathways as well as a pathway or pathways that are dependent on mitochondrial antiviral signaling protein (MAVS), IL-18Rα, IFN-γ, and PKR. Importantly, CS enhanced the effects of influenza but not other agonists of innate immunity in a similar fashion. These studies demonstrate that CS selectively […]

Cigarette smoke selectively enhances viral PAMP– and virus-induced pulmonary innate immune and remodeling responses in mice

Min-Jong Kang,[1] Chun Geun Lee,[1] Jae-Young Lee,[1] Charles S. Dela Cruz,[1] Zhijian J. Chen,[2] Richard Enelow,[1] and Jack A. Elias[1,3]

[1]Section of Pulmonary and Critical Care Medicine, Yale University School of Medicine, New Haven, Connecticut, USA.
[2]Howard Hughes Medical Institute, Department of Molecular Biology, University of Texas Southwestern Medical Center, Dallas, Texas, USA.
[3]Department of Internal Medicine, Yale University School of Medicine, New Haven, Connecticut, USA.

Viral infections have more severe consequences in patients who have been exposed to cigarette smoke (CS) than in those not exposed to CS. For example, in chronic obstructive pulmonary disease (COPD), viruses cause more severe disease exacerbation, heightened inflammation, and accelerated loss of lung function compared with other causes of disease exacerbation. Symptomatology and mortality in influenza-infected smokers is also enhanced. To test the hypothesis that these outcomes are caused by CS-induced alterations in innate immunity, we defined the effects of CS on pathogen-associated molecular pattern–induced (PAMP-induced) pulmonary inflammation and remodeling in mice. CS was found to enhance parenchymal and airway inflammation and apoptosis induced by the viral PAMP poly(I:C). CS and poly(I:C) also induced accelerated emphysema and airway fibrosis. The effects of a combination of CS and poly(I:C) were associated with early induction of type I IFN and IL-18, later induction of IL-12/IL-23 p40 and IFN-γ, and the activation of double-stranded RNA-dependent protein kinase (PKR) and eukaryotic initiation factor-2α (eIF2α). Further analysis using mice lacking specific proteins indicated a role for TLR3-dependent and -independent pathways as well as a pathway or pathways that are dependent on mitochondrial antiviral signaling protein (MAVS), IL-18Rα, IFN-γ, and PKR. Importantly, CS enhanced the effects of influenza but not other agonists of innate immunity in a similar fashion. These studies demonstrate that CS selectively augments the airway and alveolar inflammatory and remodeling responses induced in the murine lung by viral PAMPs and viruses.

Introduction

Chronic obstructive pulmonary disease (COPD) is a composite term that is used for patients with emphysema and chronic bronchitis (1–3). It is the fourth leading cause of death in the world and in Western societies is impressively associated with chronic cigarette smoke (CS) exposure (2, 3). The tissues from patients with COPD are characterized by chronic inflammation, mucus metaplasia, alveolar destruction, and structural cell apoptosis (4–8). Recent studies have also highlighted the interesting observation that the airways in COPD tissues are often remodeled and fibrotic while the nearby alveoli manifest tissue rarification and septal rupture (1). The inflammation in COPD tissues is felt to be causally related to the emphysema and other pathologic alterations in the lungs from these patients (1, 2, 9, 10) and worsens with disease progression (1, 9, 10). The mechanisms that mediate these inflammatory and remodeling responses, however, are not adequately understood.

A significant amount of the morbidity and mortality in COPD is due to acute exacerbations characterized by cough, shortness of breath, sputum production, and decreases in expiratory airflow (9–13). The frequency of these exacerbations correlates with the rate of disease progression and loss of lung function as well as the overall health status of the patient (10, 11, 14, 15). Thus, exacerbations are now considered to be legitimate targets for disease therapy (10). However, the mechanisms that mediate these exacerbations and their effects on tissue inflammation and remodeling have not been adequately defined.

Recent studies have demonstrated that a variety of viruses including rhinovirus, influenza virus, and respiratory syncytial virus (RSV) are important causes of COPD exacerbations (10, 12, 13, 16–18). Compared with exacerbations due to other causes, virus-induced COPD exacerbations are more severe, last longer, and are associated with heightened airway and systemic inflammatory responses (15, 19–21). These differences cannot be attributed solely to the structural alteration in the lungs of patients with COPD because healthy smokers also experience exaggerated symptomatic responses after viral infection (22–25). In keeping with this conceptualization, viral exacerbations in patients with COPD are felt to be due to inflammatory responses that overwhelm protective antiinflammatory defenses (10, 26). Surprisingly, the mechanisms that underlie the exaggerated virus-induced responses in CS-exposed individuals with COPD have not been defined. The mechanisms that underlie the exaggerated responses that are seen in otherwise normal smokers infected with influenza have also not been elucidated.

CS is a complex mixture of over 4,500 chemicals including free radicals and oxidants (27, 28). A variety of lines of evidence suggests that innate immunity plays an important role in the respons-

Nonstandard abbreviations used: BAL, bronchoalveolar lavage; CCSP, Clara cell 10 secretory protein; COPD, chronic obstructive pulmonary disease; CS, cigarette smoke; dsRNA, double-stranded RNA; eIF2α, eukaryotic initiation factor-2α; GDQ, gardiquimod; IHC, immunohistochemistry; IL-18Rα, IL-18 receptor α; IMQ, imiquimod; MAVS, mitochondrial antiviral signaling protein; Mda5, melanoma differentiation–associated protein-5; PAMP, pathogen-associated molecular pattern; PARP, poly(ADP-ribose) polymerase; PKR, double-stranded RNA-dependent protein kinase; poly(I:C), polyinosine-polycytidylic acid; RA, room air; RIG-1, retinoic acid–inducible gene-1; RSV, respiratory syncytial virus; VSV, vesicular stomatitis virus.

Conflict of interest: The authors have declared that no conflict of interest exists.

Citation for this article: *J. Clin. Invest.* **118**:2771–2784 (2008). doi:10.1172/JCI32709.

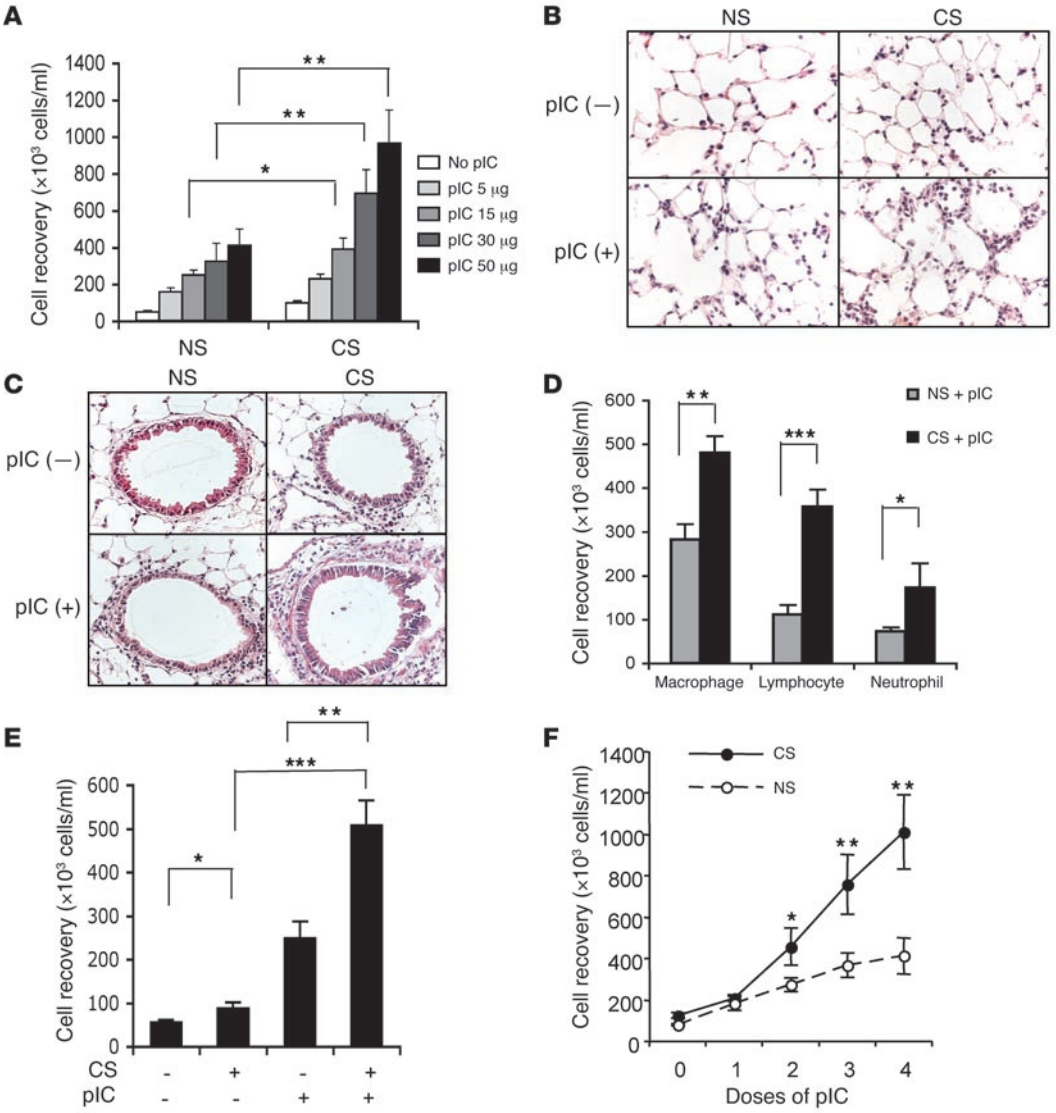

Figure 1

Inflammatory effects of poly(I:C) in mice exposed to RA or CS. C57BL/6J mice were exposed to CS or RA (NS, nonsmoking) for 2 weeks and then randomized to receive 4 doses of poly(I:C) [pIC+] or vehicle control [pIC–]. The effects of 4 doses of varying concentrations of poly(I:C) on BAL total cell recovery (**A**), 4 doses of poly(I:C) (50 μg) on parenchymal (**B**) and airway (**C**) inflammation, and BAL differential cell recovery (**D**) are illustrated. (**E**) Effects of 4 doses of poly(I:C) on BALB/c mice breathing RA (CS–) and mice exposed to CS (CS+) are illustrated. (**F**) Dose dependence of these inflammatory events in C57BL/6J mice. The values in parts **A**, **D**, **E**, and **F** represent the mean ± SEM of evaluations in a minimum of 5 mice. Parts **B** and **C** are representative of a minimum of 4 similar experiments. *$P < 0.05$; **$P < 0.01$; ***$P < 0.001$. Original magnification, ×20.

es to and clearance of these agents. This includes the well-known ability of CS to increase the number of innate immune effectors such as neutrophils and macrophages in the lung and the demonstration that CS regulates macrophage function and the expression of genes involved in innate immune responses (29–32). Recent studies have also demonstrated that an adaptive immune response is not a prerequisite for the generation of CS-induced emphysema (29). These observations led to the hypothesis that the innate immune response plays a particularly important role in the pathogenesis of the inflammatory and remodeling responses in CS-exposed individuals (33). However, the innate immune pathways that are involved in these responses and the pathogen-associated molecular patterns (PAMPs) that trigger these responses have not been defined. The importance of innate immunity in the pathogenesis of COPD exacerbations and virus-induced inflammation and remodeling have also not been addressed.

We hypothesized that CS selectively alters innate immune responses in the lung and that these alterations contribute to the pathogenesis of COPD and other CS- and virus-associated disorders. To test this hypothesis, we evaluated the function of COPD-relevant innate immune pathways in mice that have been exposed to CS or room air (RA). Because viral and virus-like responses can be triggered by pathways involving TLRs and or RNA helicases and mediated via the activation of double-stranded RNA-dependent (dsRNA-dependent) protein kinase (PKR), each of these was evaluated in these studies. These studies demonstrate that CS

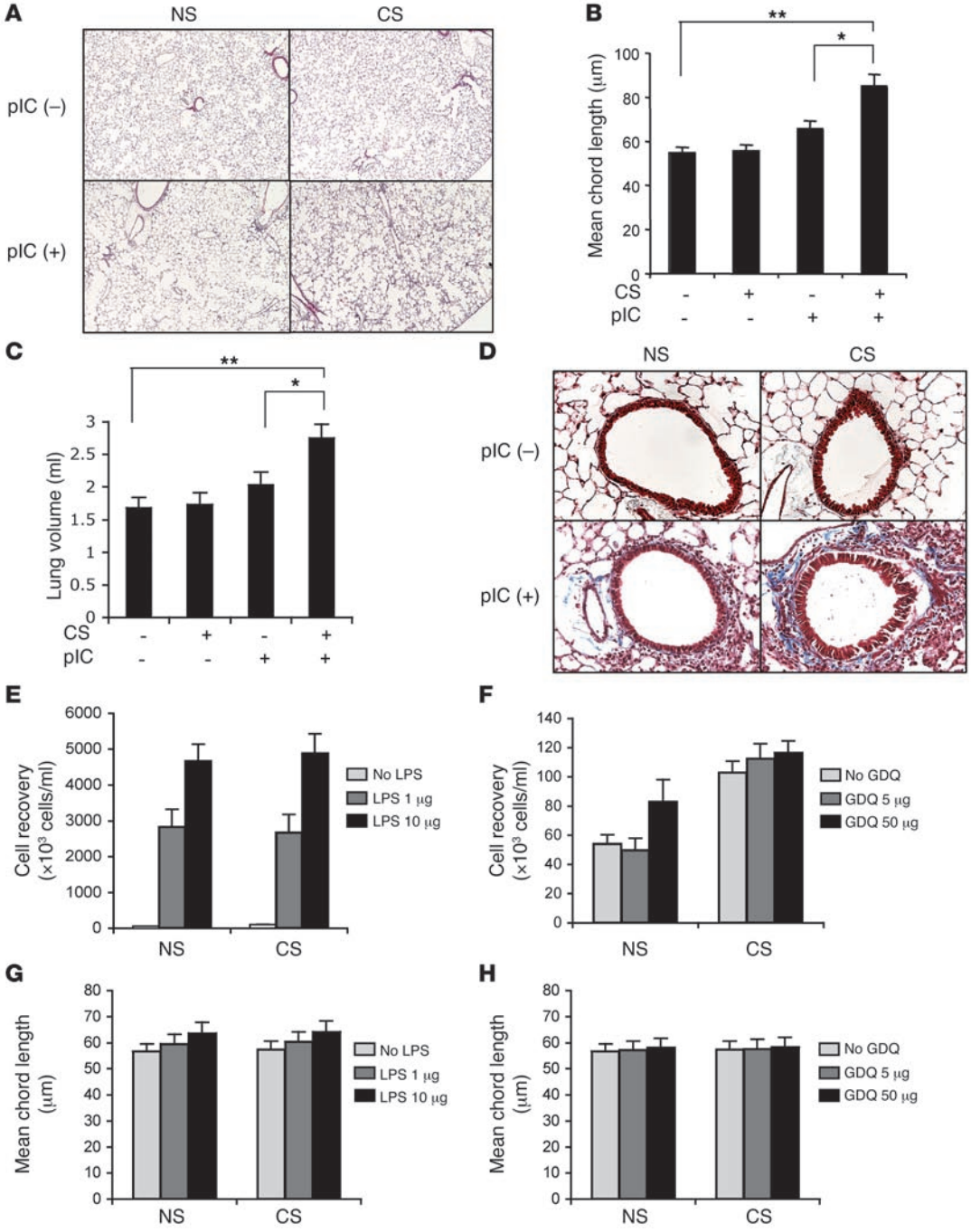

Figure 2

Effects of poly(I:C) and other innate immunity agonists on mice exposed to RA or CS. Mice were exposed to CS or RA for 2 weeks and then randomized to receive 4 doses of poly(I:C) (50 μg), LPS (1–10 μg), GDQ (5–50 μg), or vehicle controls. The alterations in alveolar structure, alveolar chord length, and lung volume caused by poly(I:C) are noted in parts **A**, **B**, and **C**. The effects of these interventions on matrix accumulation were assessed with trichrome evaluations (**D**). The effects of LPS and GDQ on BAL inflammation are seen in **E** and **F**. The effects of LPS and GDQ on alveolar remodeling are illustrated in parts **G** and **H**, respectively. The values in **B**, **C**, and **E**–**H** represent the mean ± SEM of evaluations in a minimum of 5 mice. Parts **A** and **C** are representative of a minimum of 4 similar experiments. **P* < 0.05; ***P* < 0.01. Original magnification, ×4 (**A**); ×20 (**D**).

selectively augments the inflammatory and remodeling responses produced by viral PAMPs and influenza virus. They also highlight the specificity of and define the mechanisms that mediate these important responses.

Results

Inflammatory effects of poly(I:C) in CS-exposed mice. To begin to characterize the effects of CS on innate immune responses in the lung, we compared the responses induced by ligands that activate known

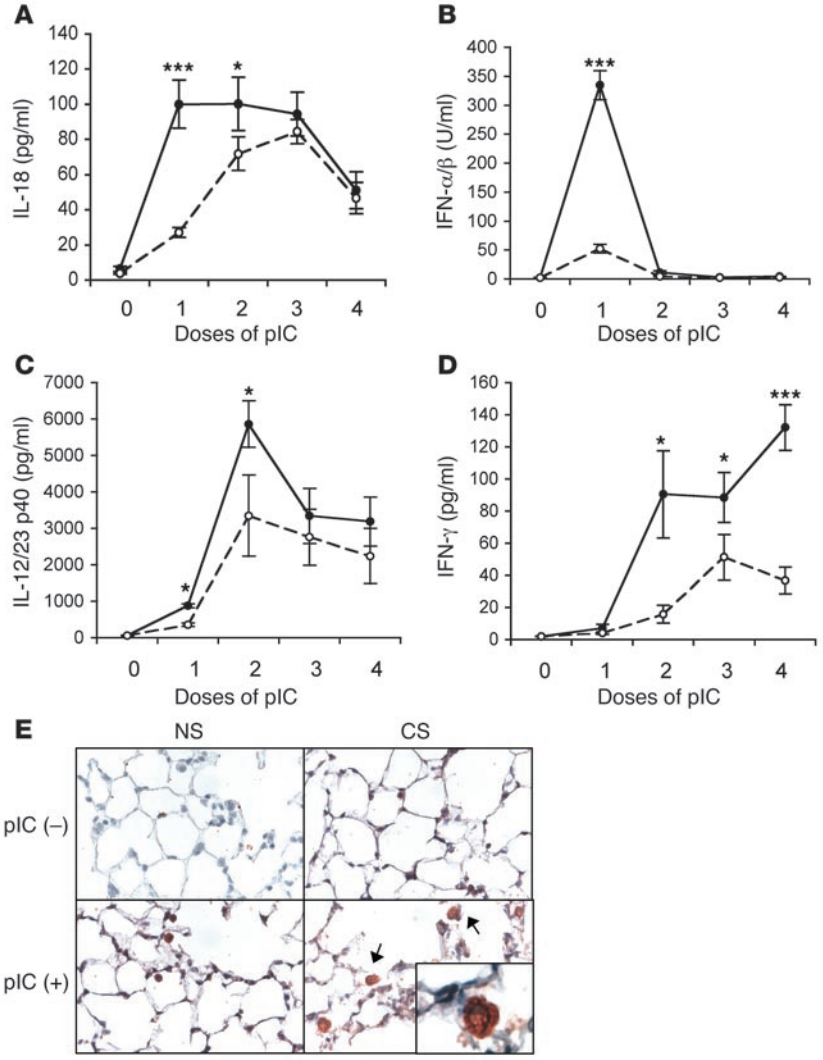

Figure 3
Effects of poly(I:C) on cytokines and IFNs. Mice were exposed to CS or RA for 2 weeks and then randomized to receive poly(I:C) (50 μg) or vehicle control. The levels of BAL IL-18, IFN-α/β, IL-12/IL-23 p40, and IFN-γ in vehicle-treated mice breathing RA or CS were near or below the limits of detection of these assays. The effects of poly(I:C) in mice exposed to CS (filled circles) or RA (open circles) are illustrated (**A**–**D**). The localization of IL-18 was accomplished using IHC (**E**). In the lungs from mice exposed to CS plus poly(I:C), selected IL-18–containing macrophages are highlighted with arrows, and a high-power image can be seen in the insert. The values in parts **A**–**D** represent the mean ± SEM of evaluations in a minimum of 5 mice. Part **E** is representative of 3 similar experiments. *$P < 0.05$; ***$P < 0.001$. Original magnification, ×20 (**E**); ×100 (insert).

innate immune pathways in C57BL/6J mice breathing RA and mice exposed to CS for varying intervals. dsRNA (polyinosine-polycytidylic acid [poly(I:C)]) was initially chosen in an attempt to define responses that could be elicited by viral infections. CS exposure caused modest increases in bronchoalveolar lavage (BAL) total cell and neutrophil recovery (Figure 1A and data not shown). It also caused scattered foci of neutrophilic inflammation in lungs from some but not all mice (Figure 1, B and C, and data not shown). In contrast, poly(I:C) caused significant increases in total cell, macrophage, lymphocyte, and neutrophil recovery and a neutrophil- and macrophage-rich tissue inflammatory response (Figure 1, A–D). Importantly, CS and poly(I:C) interacted in a synergistic manner to enhance this BAL, airway, and alveolar inflammation (Figure 1, A–D). Similar responses were seen in BALB/c mice (Figure 1E). This interaction was dose dependent with the most striking effects being seen when 50 μg of poly(I:C) (the highest dose tested) was given to CS-exposed mice for 2 weeks (4 doses) (Figure 1, A and F). Significant interactions were also seen with doses of poly(I:C) as low as 15 μg and after 2 aspirations of high-dose (50 μg) poly(I:C) (Figure 1, A and F). Importantly, this interaction was also time dependent, with exposures as short as 2 weeks and as long as 3 months causing comparable increases in poly(I:C)-induced inflammation and lesser effects being seen with shorter intervals of CS exposure (data not shown). In all cases, this effect was at least partially poly(I:C)-specific because similar synergy was not seen when LPS (0.01–10 μg), CpG (0.5–5 μg), gardiquimod (GDQ) (5–50 μg), or imiquimod (IMQ) (10–100 μg) were administered in a similar fashion (data not shown). It also required CS and poly(I:C) because LPS did not interact in a similar manner with poly(I:C) and the repeated administration of poly(I:C) alone for up to 3 months did not induce comparable tissue effects (data not shown). These studies demonstrate that CS selectively enhances the alveolar and airway inflammatory effects of poly(I:C) in the murine lung.

Remodeling responses induced by poly(I:C) in CS-exposed mice. To gain insight into the functional consequences of the interaction noted above, we compared the lung tissues in C57BL/6J mice breathing RA and mice that had been exposed to CS for 2 weeks prior to poly(I:C) administration. At this time point, CS alone did not cause a significant increase in alveolar size and 4 doses of poly(I:C) in RA-exposed mice caused an increase that did not achieve statistical significance (Figure 2, A and B). In contrast, impressive alveolar remodeling with emphysematous alterations on light microscopic examination and significant increases in morphometrically determined alveolar chord length were noted in CS-exposed mice that

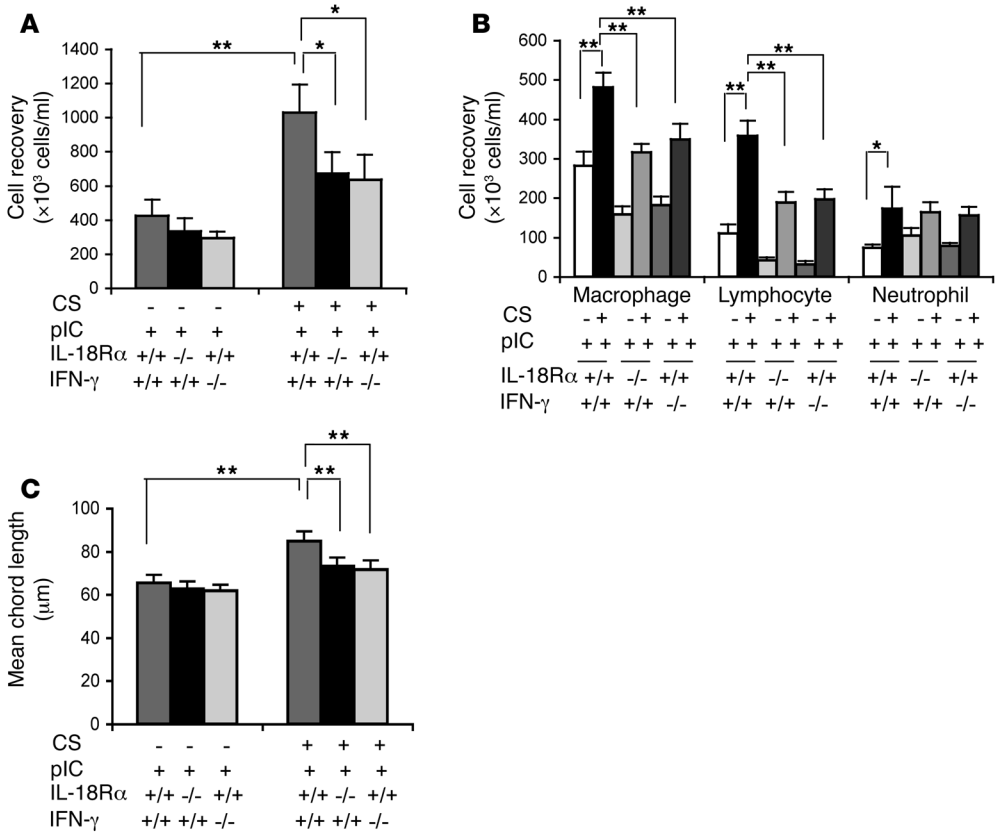

Figure 4
Roles of IL-18Rα and IFN-γ in the interaction of CS and poly(I:C). WT (+/+) mice and mice with null mutations (–/–) of IL-18Rα or IFN-γ were exposed to CS or RA (CS–) for 2 weeks and then given 4 doses of poly(I:C) (50 μg) or vehicle control. BAL total cell recovery (**A**), BAL differential cell recovery (**B**), and emphysema (**C**) were evaluated. The noted values represent the mean ± SEM of evaluations in a minimum of 5 mice. $^{*}P < 0.05$; $^{**}P < 0.01$.

received 4 doses of poly(I:C) (Figure 2, A and B). The lungs from mice exposed to CS plus poly(I:C) also manifested increased lung volumes after pressure fixation (Figure 2C). Similar responses were also seen in BALB/c mice (data not shown). In addition, these alveolar alterations were associated with a fibrotic airway remodeling response that was detectable on trichrome histologic evaluation (Figure 2D). In all cases, these interactions were dose and time dependent and could be observed with doses of poly(I:C) as low as 15 μg and after as few as 2 doses of high-concentration poly(I:C) (data not shown). They were also at least partially poly(I:C)-specific because LPS, CpG, GDQ, and IMQ did not have similar effects (Figure 2, E–H, and data not shown). Finally, they also required CS plus poly(I:C) because LPS did not interact in a similar fashion with poly(I:C) and repeat dosing with poly(I:C) alone for up to 3 months did not induce similar remodeling responses (data not shown). Thus, in addition to its ability to enhance inflammation, CS selectively enhances the ability of poly(I:C) to induce pulmonary emphysema and airway remodeling.

Regulation of IL-18, IL-12, and type I and type II interferons. In keeping with their roles in viral responses and COPD, we next evaluated the production of IL-18, IL-12/IL-23 p40, and type I and type II IFNs in this modeling system. In these experiments, the vehicle controls did not stimulate the production of any of these cytokines (data not shown). In contrast, poly(I:C) was a potent stimulator of BAL IL-18, IL-12/IL-23 p40, and type I and type II IFNs (Figure 3, A–D). Importantly, these inductive responses were significantly greater in mice exposed to CS compared with mice in RA (Figure 3, A–D). In all cases, these inductive events had distinct kinetic patterns with IL-18 and type I IFNs being induced early [after a single dose of poly(I:C)], IL-12/IL-23 p40 being seen with an intermediate kinetic [after 2-3 doses of poly(I:C)], and IFN-γ being induced later [after 3-4 doses of poly(I:C)] (Figure 3, A–D). Similar inductive responses were not seen when CS-exposed animals were treated with LPS, CpG, GDQ, or IMQ (data not shown). Thus, the ability of CS to selectively enhance poly(I:C)-induced inflammation and alveolar remodeling is associated with the enhanced production of IL-18, IL-12/IL-23 p40, IFN-γ, and type I IFNs.

To further define these cytokine responses, immunohistochemistry (IHC) was used to localize the IL-18 in our modeling system. In accord with previous reports from our laboratory (34), IL-18 was detected in airway epithelial cells and alveolar type 2 cells in lungs from WT mice (Figure 3E and data not shown). Low levels of IL-18 were also appreciated in alveolar macrophages from these animals (Figure 3E). In mice exposed to CS plus poly(I:C), increased levels of IL-18 were observed. This was most prominent in the alveolar macrophages, with lesser increases being noted in the alveolar and airway epithelial populations (Figure 3E and data not shown). This demonstrates that alveolar macrophages are the major site of IL-18 augmentation in CS plus poly(I:C)–treated mice.

Roles of IL-18Rα and IFN-γ. The roles of IL-18 and IFN-γ were subsequently evaluated by comparing the inflammatory, emphysematous, and cytokine responses induced by CS plus poly(I:C) in mice with WT and null IL-18 receptor α (IL-18Rα) or IFN-γ loci. In these experiments CS plus poly(I:C) induction of BAL inflammation, macrophage and lymphocyte accumulation, tissue inflammation, and alveolar remodeling were significantly diminished in mice with null mutations of IL-18Rα or IFN-γ (Figure 4, A–C, and data not shown). Thus, IL-18Rα and IFN-γ play critical roles in the pathogenesis of the inflammation and remodeling that is induced by CS plus poly(I:C).

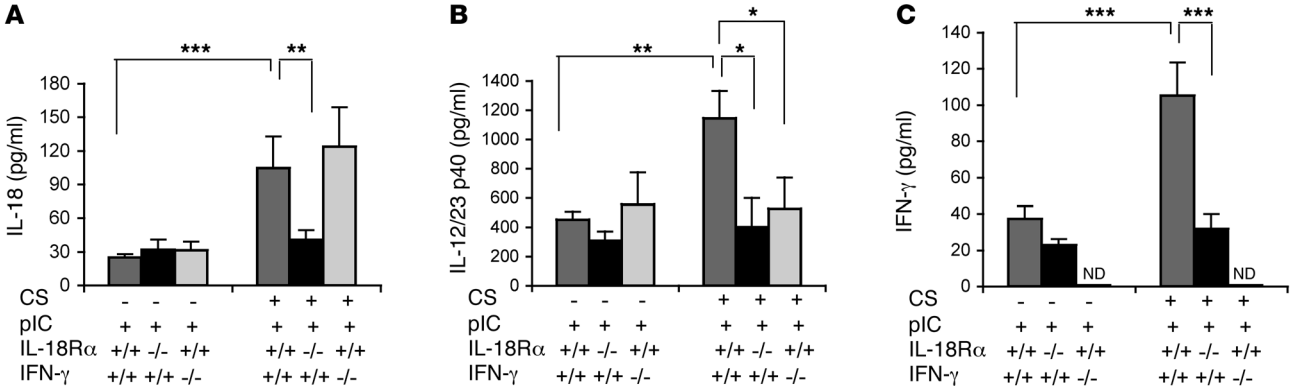

Figure 5
Roles of IL-18Rα and IFN-γ in CS plus poly(I:C)–induced cytokine stimulation. WT (+/+) mice and mice with null mutations (–/–) of IL-18Rα or IFN-γ were exposed to CS or RA (CS–) for 2 weeks and then given 1 (**A** and **B**) or 4 doses (**C**) of poly(I:C) (50 μg) or vehicle control. BAL IL-18 (**A**), IL-12/IL-23 p40 (**B**), and IFN-γ (**C**) levels were quantitated. The noted values represent the mean ± SEM of evaluations in a minimum of 5 mice. *$P < 0.05$; **$P < 0.01$; ***$P < 0.001$. ND, none detected.

Cytokine-cytokine interactions. Studies were also undertaken to define the relationships between the cytokines that were induced in this modeling system. Interestingly, in the absence of IL-18Rα, the ability of CS plus poly(I:C) to stimulate the production of IL-18, IL-12/IL-23 p40, and IFN-γ were significantly diminished (Figure 5, A–C). In contrast, in the absence of IFN-γ, the induction of IL-18 was not altered while the induction of IL-12/IL-23 p40 was significantly decreased (Figure 5, A and B). These studies highlight a cytokine receptor cascade in which IL-18 receptor signaling is a proximal event that plays a critical role in the induction of IL-12/IL-23 p40 and IFN-γ, IL-18 is autoinduced via an IL-18Rα–dependent mechanism, and IFN-γ contributes to the induction of IL-12/IL-23 p40 but not IL-18.

Roles of TLR3. To define the innate immunity pathway or pathways that are involved in the interaction of CS and poly(I:C), we evaluated the consequences of an acute challenge with poly(I:C) (1 dose) or repeated challenges with poly(I:C) (4 doses) in mice exposed to RA and CS with WT and null TLR3 loci. In mice given 1 dose of poly(I:C) and evaluated 4 days later, a modest decrease in BAL and tissue inflammation was noted in comparisons of TLR3-deficient and WT animals (Figure 6A). In contrast, TLR3-null and WT animals exposed to CS and 4 doses of poly(I:C) had a similar ability to stimulate IFN-γ, induce BAL and tissue inflammation, and induce alveolar remodeling (see Figure 6, B–D, and data not shown). Thus, TLR3 plays a small role in the pathogenesis of the acute responses induced by poly(I:C) in CS-exposed mice while repeated doses of poly(I:C) induce inflammation and alveolar remodeling via a pathway or pathways that are largely TLR3 independent.

Role of mitochondrial antiviral signaling protein in responses induced by CS plus poly(I:C). To further define the innate pathways that mediate the interactions of CS plus poly(I:C), we compared the inflammation, cytokine responses, and alveolar remodeling in WT mice with that of mice with null mutations of the mitochondrial antiviral signaling protein MAVS. MAVS was chosen because it links RNA helicases like retinoic acid–inducible gene-1 (RIG-1) and melanoma differentiation–associated protein-5

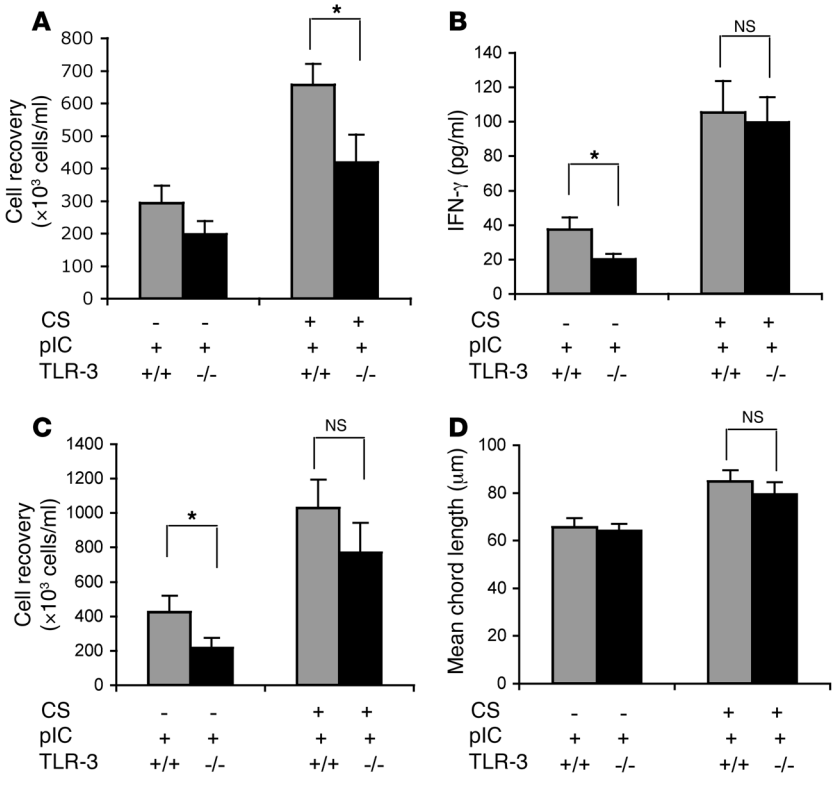

Figure 6
Roles of TLR3 in the interaction of CS and poly(I:C). WT (+/+) mice and mice with null mutations (–/–) of TLR3 were exposed to CS or RA (CS–) for 2 weeks and then given 1 or 4 doses of poly(I:C) (50 μg) or vehicle control. BAL total cell recovery after a single dose of poly(I:C) is illustrated in **A**. The levels of BAL IFN-γ (**B**), BAL total cell recovery (**C**), and alveolar remodeling (**D**) after 4 doses of poly(I:C) were also evaluated. The noted values represent the mean ± SEM of evaluations in a minimum of 5 mice. *$P < 0.05$.

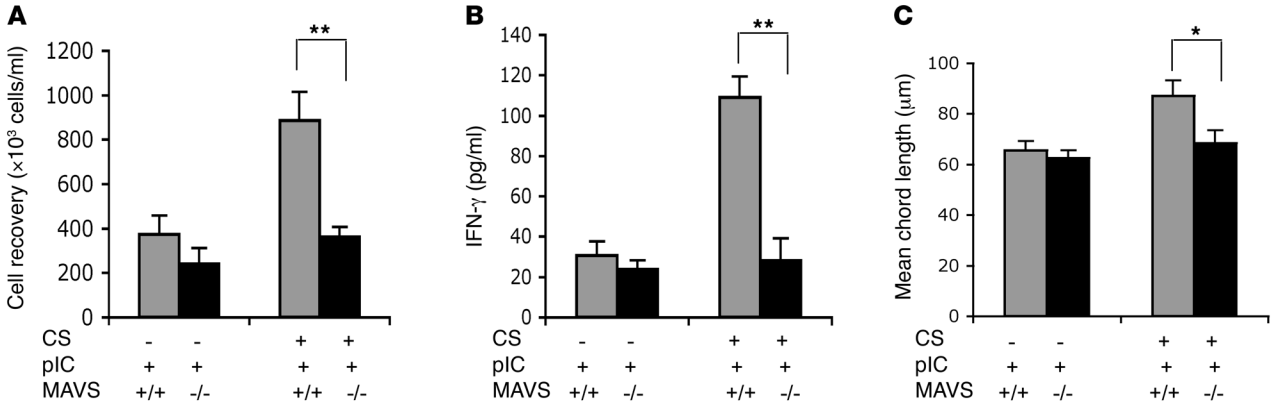

Figure 7
Roles of MAVS in the interaction of CS and poly(I:C). WT (+/+) mice and mice with null mutations (–/–) of MAVS were exposed to CS or RA (CS–) for 2 weeks and then given 4 doses of poly(I:C) (50 μg) or vehicle control. BAL total cell recovery (**A**), IFN-γ production (**B**), and alveolar remodeling (**C**) were evaluated. The noted values represent the mean ± SEM of evaluations in a minimum of 5 mice. *$P < 0.05$; **$P < 0.01$.

(Mda5) to antiviral effector responses (35, 36). These studies demonstrated that MAVS plays a critical role in these responses because the inflammatory, cytokine-inductive, and remodeling responses induced by poly(I:C) in CS-exposed mice were abrogated in MAVS-deficient animals (Figure 7, A–C). This demonstrates that a MAVS-related pathway plays a major role in the interaction of CS and poly(I:C).

Regulation and roles of PKR. Studies were next undertaken to evaluate the activation of PKR in our experimental system. As shown in Figure 8A, phosphorylated PKR was not observed or was present in only modest quantities in lungs from mice in RA, mice exposed to CS only, and mice treated with just poly(I:C). In contrast, the activation of PKR was greatly enhanced in mice exposed to CS prior to poly(I:C) administration (Figure 8A). These inductive events were dose and time dependent, being seen after as little as 2 inhalations of high-dose poly(I:C) and with doses of poly(I:C) as low as 15 μg/ml (data not shown). They were also mediated by pathways that are at least partially IL-18Rα– and IFN-γ–dependent because PKR phosphorylation was significantly diminished in IL-18Rα–null and IFN-γ–null animals (Figure 8B). These activation events were also downstream of MAVS because the ability of poly(I:C) to activate PKR in CS-exposed mice was significantly decreased in MAVS-null mice (Figure 8C).

The functional consequences of PKR activation were next evaluated by comparing the effects of CS plus poly(I:C) in mice with WT and null PKR loci. These studies demonstrated that the inflammatory and alveolar remodeling effects of poly(I:C) in CS-exposed mice were significantly diminished in animals with null mutations of PKR (Figure 8, D–F). In contrast, null mutations of PKR did not alter the production of IL-18 or IFN-γ in mice treated with CS plus poly(I:C) (see Supplemental Figures 1 and 2; supplemental material available online with this article; doi:10.1172/JCI32709DS1). When viewed in combination, these studies demonstrate that PKR is activated via a MAVS-, IL-18Rα–, and IFN-γ–dependent mechanism or mechanisms in CS-exposed mice treated with poly(I:C) and that this activation plays an essential role in the pathogenesis of the enhanced inflammatory and emphysematous responses in these animals. They also demonstrate that PKR does not play a role in the enhanced induction of IL-18 or IFN-γ, suggesting that PKR activation is distal to IFN-γ in this effector cascade.

Apoptosis in poly(I:C)-treated CS-exposed animals. In keeping with the importance of structural cell apoptosis in CS-induced emphysema (7, 8, 37–39), studies were undertaken to evaluate the DNA injury and cell death responses in our experimental system. These studies demonstrated that CS alone and poly(I:C) administration to mice breathing RA each caused small but significant increases in the number of cells that were TUNEL stain positive (Figure 9A). In contrast, a significant increase in the number of TUNEL-positive cells was seen in the parenchyma and airways of CS-exposed mice that were treated with poly(I:C) (Figure 9A and data not shown). Double-label IHC demonstrated significant increases in the percentages of pro–SP-C$^+$ alveolar epithelial cells, CD31$^+$ endothelial cells, and Clara cell 10 secretory protein$^+$ (CCSP$^+$) airway epithelial cells in lungs from mice incubated with CS plus poly(I:C) (Figure 9B and Supplemental Figure 3). In contrast, less than 20% of the TUNEL cells were CD3$^+$ or F4/80$^+$ (data not shown). Caspase-3 activation, cleavage of the caspase target poly(ADP-ribose) polymerase (PARP), and phosphorylation of eukaryotic initiation factor-2α (eIF2α), a major PKR target that plays an important role in a variety of apoptotic responses (40–43), were not noted or were weakly detectable in lungs from mice breathing RA, CS-exposed mice, and mice that received only poly(I:C) (Figure 9C). In accord with our TUNEL findings, each of these responses was detected in significantly enhanced quantities in mice exposed to CS plus poly(I:C) (Figure 9C). This DNA injury and cell death response was mediated via a MAVS-, IL-18Rα–, IFN-γ–, and PKR-dependent mechanism or mechanisms, since the levels of TUNEL staining, eIF2α phosphorylation, and caspase-3 activation were significantly diminished in poly(I:C) plus CS–treated mice with null mutations of MAVS, IL-18Rα, IFN-γ, or PKR, respectively (Figure 9, D–G, and data not shown). These studies demonstrate that CS enhances the ability of poly(I:C) to induce epithelial and endothelial cell DNA injury, cell death, and caspase and eIF2α activation. They also highlight important roles that MAVS, IL-18Rα, IFN-γ, and PKR play in these apoptotic responses.

Effects of influenza in CS-exposed mice. The studies noted above used poly(I:C) as a surrogate for dsRNA viruses and single-stranded RNA viruses that go through a double-stranded stage during viral replication. To begin to evaluate the validity of this assumption, we compared the effects of influenza virus in mice exposed to RA or CS for

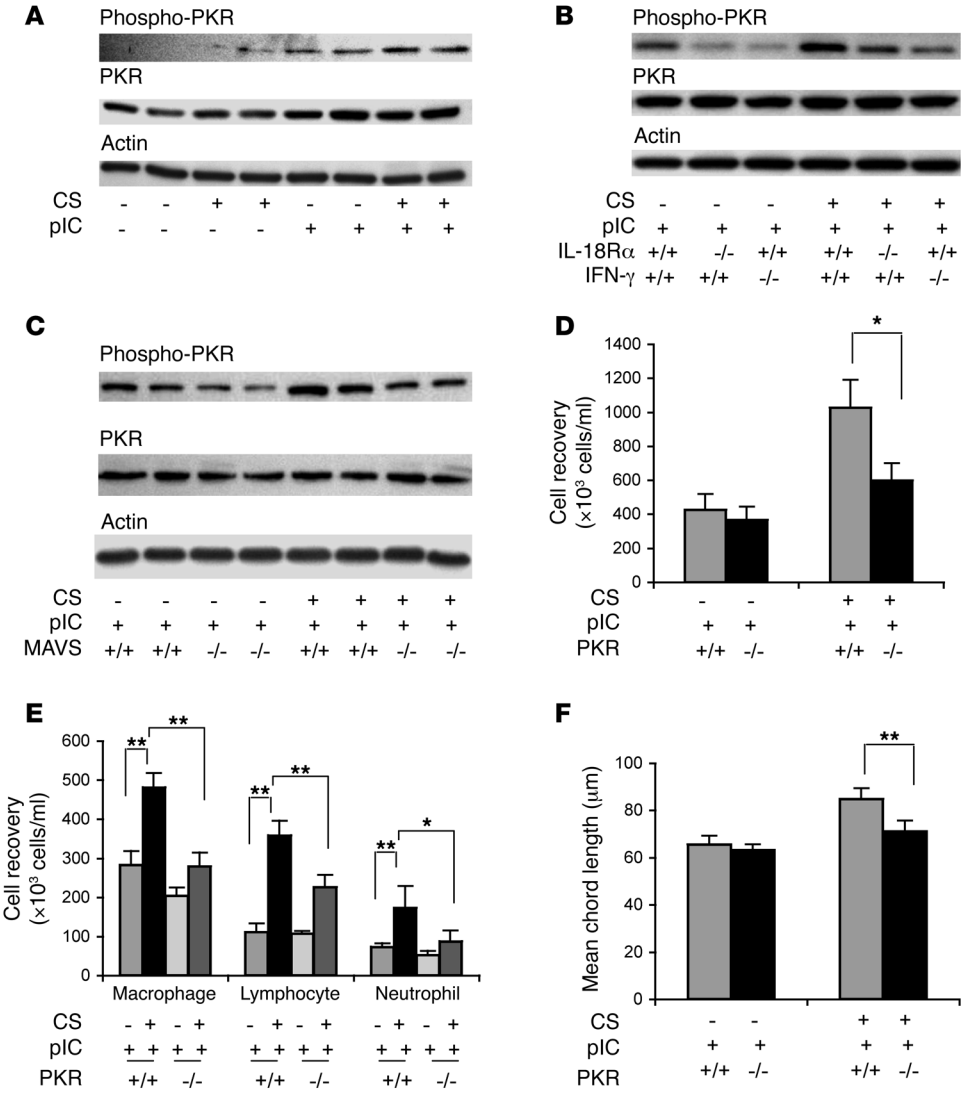

Figure 8
Regulation and roles of PKR in the interaction of CS and poly(I:C). Mice were exposed to CS or RA (CS–) for 2 weeks and then given 4 doses of poly(I:C) (50 μg) or vehicle control. (**A**) Effects of poly(I:C) on PKR phosphorylation. The roles of IL-18Rα and IFN-γ in this activation are seen in comparisons of the levels of PKR phosphorylation in WT (+/+) mice and mice with null (–/–) mutations of IL-18Rα or IFN-γ (**B**). The role or roles of MAVS in this activation are seen in comparisons of the levels of PKR phosphorylation in WT (+/+) mice and mice with null (–/–) mutations of MAVS (**C**). The roles of PKR in poly(I:C)-induced total (**D**) and differential (**E**) BAL cell recovery and emphysema (**F**) are also illustrated. The values in parts **D**–**F** represent the mean ± SEM of evaluations in a minimum of 5 mice. The data depicted in each row in parts **A**–**C** were generated from blots of individual gels that were run at the same time. Parts **A**–**C** are representative of a minimum of 3 similar evaluations. *$P < 0.05$; **$P < 0.01$.

2 weeks prior to infection. In mice breathing RA, influenza infection caused alveolar, airway, and BAL inflammatory responses characterized by increases in total cell, neutrophil, lymphocyte, and macrophage accumulation that peaked 9 days after inoculation (Figure 10, A–C). This response was associated with modest increases in the production of IL-18 (Figure 10D), IL-12/IL-23 p40 (Figure 10E), and IFN-γ (Figure 10F); modest levels of caspase 3 activation, PARP cleavage, and PKR and eIF2α activation (Figure 10G); and low levels of TUNEL staining (Figure 10H). Emphysematous alveolar remodeling was not noted (Figure 10I). In accordance with our findings with poly(I:C), each of these responses was exaggerated in CS-exposed mice infected with influenza (Figure 10, A–H). Influenza infection also induced emphysematous alveolar remodeling and increased the levels of apoptosis in SP-C$^+$ and CD31$^+$ cells in CS-exposed animals (Figure 10I and data not shown). These studies demonstrate that CS enhances the inflammatory, remodeling, and apoptotic effects of influenza in the lung and highlight the induction of IL-18, IL-12/IL-23 p40, and IFN-γ and activation of PKR and eIF2α in this setting.

Pathways in CS-influenza interaction. To define the mechanisms that underlie these responses, we compared the effects of influenza in CS-exposed mice with null mutations of IL-18Rα, TLR3, and PKR. In accordance with our findings with poly(I:C), IL-18R signaling played an important role in the inflammation, alveolar remodeling, and apoptosis induced by influenza in CS-exposed mice (Figure 11, A–D). TLR3 also played a role in the inflammation and remodeling in CS-exposed, influenza-infected mice (Figure 11, A–D). Interestingly, the contributions of PKR were more complex with CS plus influenza–induced inflammation being mediated by PKR-independent and alveolar remodeling and apoptosis being mediated by PKR-dependent pathways (Figure 11, A–E). Importantly, these augmented virus-induced responses could not be attributed to differences in viral clearance because similar viral loads were seen in lungs from mice breathing RA and CS at all time points (data not shown). These studies demonstrate that IL-18Rα, TLR3, and PKR play important roles in the inflammatory and remodeling responses induced by CS plus influenza.

Discussion

To determine whether CS alters innate immune responses in the lung, we compared the inflammatory and remodeling responses induced by innate immunity agonist PAMPs in mice breathing RA and mice exposed to CS. These studies demonstrate that CS has a

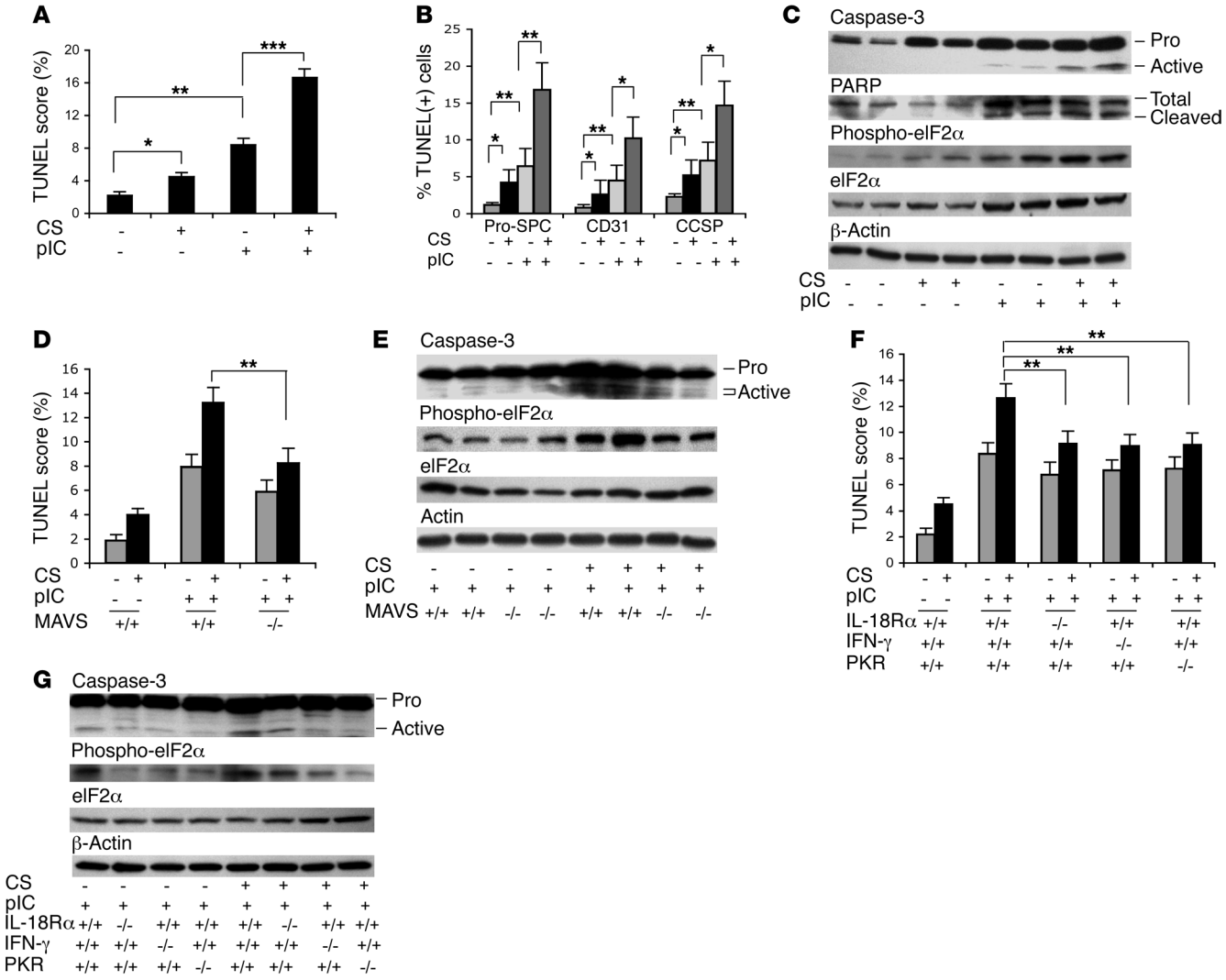

Figure 9

Effects of CS and poly(I:C) on cellular apoptosis. Mice were exposed to CS or RA (CS–) for 2 weeks and then given 4 doses of poly(I:C) (50 μg) or vehicle control. The effects of these interventions on the percentage of alveolar structural cells that were TUNEL stained (+) can be seen in **A**. Double-label IHC was used to define the percentage of pro–SP-C–positive alveolar type II cells, CD31-positive endothelial cells, and CCSP-positive airway epithelial cells that were TUNEL stained, respectively (**B**). The effects of CS and poly(I:C) on caspase-3 activation, PARP accumulation and activation, and eIF2α accumulation and activation were also assessed (**C**). The role of MAVS was assessed by comparing the levels of TUNEL staining, phosphorylation of eIF2α, and caspase-3 activation in WT mice (+/+) and mice with null (–/–) mutations of MAVS (**D** and **E**). The roles of IL-18Rα, IFN-γ, and PKR were assessed by comparing these responses in WT mice (+/+) and mice with null (–/–) mutations of IL-18Rα, IFN-γ, or PKR (**F** and **G**). The data in each row in parts **C**, **E**, and **G** were generated from blots of individual gels that were run at the same time. Parts **C**, **E**, and **G** are representative of a minimum of 3 similar evaluations. The values in parts **A**, **B**, **D**, and **F** represent the mean ± SEM of evaluations in a minimum of 5 mice. $^{*}P < 0.05$; $^{**}P < 0.01$; $^{***}P < 0.001$.

remarkable and selective effect on these responses. Specifically, they demonstrate in 2 different murine strains that CS selectively enhances the airway and parenchymal inflammatory, remodeling, and apoptotic responses induced by the viral PAMP dsRNA. The studies also demonstrate that this interaction is associated with the early induction of type I IFNs and IL-18, later induction of IL-12/IL-23 p40 and IFN-γ, and the activation of PKR and eIF2α. They also highlight the TLR 3-dependent and -independent, MAVS-dependent, and IL-18Rα–, IFN-γ– and PKR-dependent mechanisms that contribute to these events. The viral relevance of these findings was also defined by demonstrating that CS interacts in a similar fashion with influenza to increase inflammation, apoptosis and emphysema, and IL-18 and IFN-γ production and to activate PKR. Finally, these studies also defined the important roles that TLR3, IL-18Rα, and PKR play in these virus-CS–induced responses. We believe these are the first studies to define the CS-induced alterations in virus-related innate immune responses in the lung, the first to demonstrate that exaggerated inflammatory and remodeling responses are seen when CS and viral PAMPs or live viruses are combined, and the first to define the pathways that mediate these responses. These studies provide insight into the mechanisms that can contribute to virus-induced COPD exacerbations and the impressive symp-

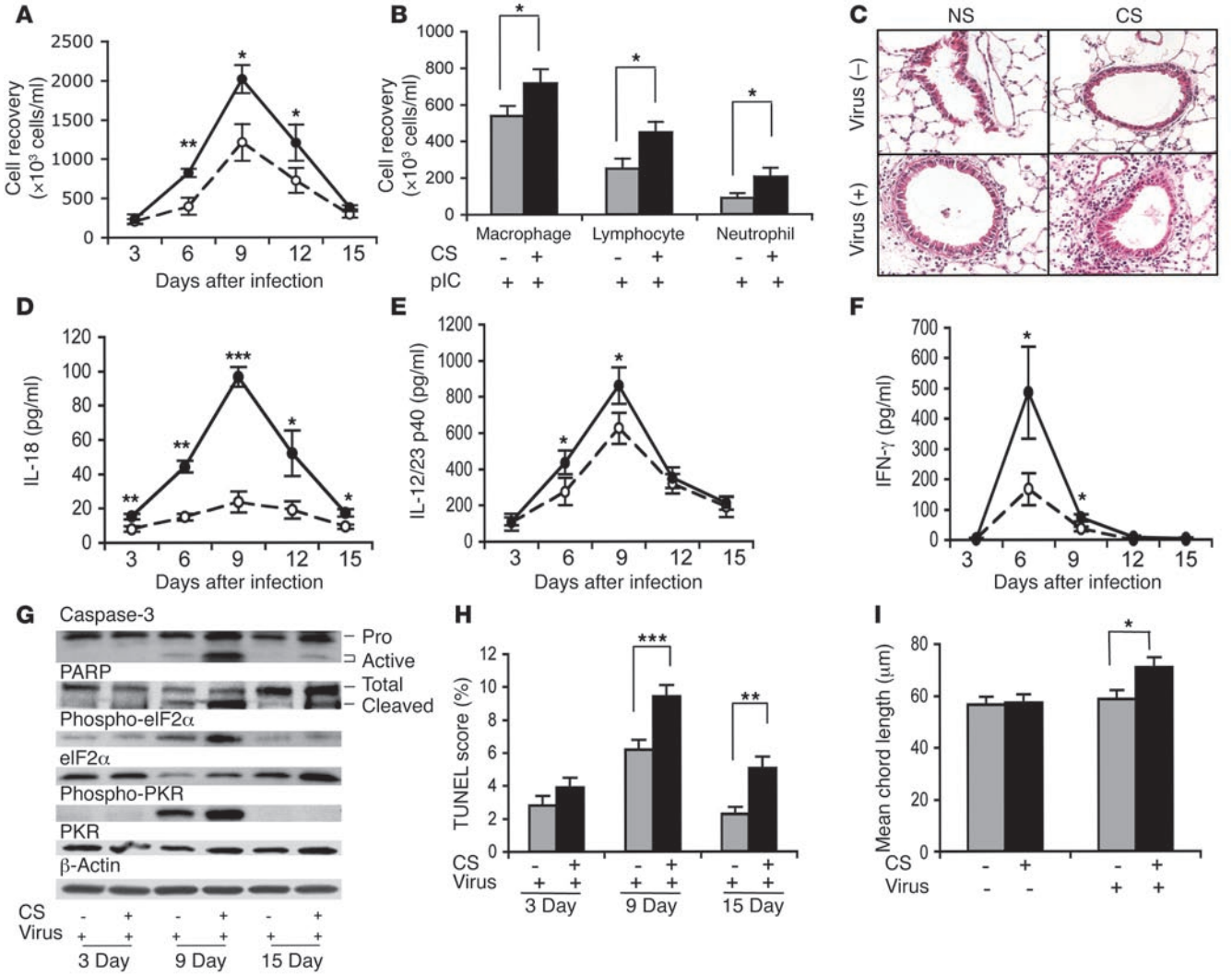

Figure 10

Interactions of influenza virus and CS. Mice were exposed to CS or RA (CS–) for 2 weeks and then infected with influenza virus (virus+) or vehicle control (virus–). The effects of this intervention on total BAL cell recovery (**A**), differential cell recovery (9 days after infection) (**B**), tissue inflammation (**C**), and levels of BAL IL-18 (**D**), BAL IL-12/IL-23 p40 (**E**), and BAL IFN-γ (**F**) are compared in mice exposed to RA (open circles) and CS (filled circles). The effects of this intervention on caspase-3 activation, PARP cleavage, and PKR and eIF2α phosphorylation (**G**), cellular apoptosis (**H**), and alveolar remodeling (15 days after infection) (**I**) were also assessed. The values in parts **A**, **B**, **D**–**F**, **H**, and **I** represent the mean ± SEM of evaluations in a minimum of 5 mice. That data in each row in part **G** were generated from blots of individual gels that were run at the same time. Parts **C** and **G** are representative of 3 similar evaluations. $^{*}P < 0.05$; $^{**}P < 0.01$; $^{***}P < 0.001$. Original magnification, ×20.

tomatology and loss of lung function that are noted in this setting (10, 11, 15, 19–21). They also provide insight into the mechanisms that can contribute to the exaggerated severity of viral infections in otherwise healthy smokers (22–25) and highlight targets against which therapies can be directed to control virus-induced responses in smokers with and without COPD.

In studies that have focused largely on bacterial stimuli, CS and its components, such as nicotine, have been shown to have immunosuppressive properties including the ability to inhibit macrophage function (reviewed in ref. 28). Surprisingly, these lesions have been extrapolated to viruses despite preliminary studies that suggest that viral responses may be different (44). Our studies demonstrate that the concept that CS is strictly immunosuppressive is not correct. Specifically, we demonstrate that in the case of viral PAMPs and live virus, CS enhances immune responses and the tissue consequences of these responses. They also highlight the impressive specificity of this interaction by demonstrating that a variety of other innate immunity agonists do not interact with CS in a similar manner, cannot replace CS in this experimental system, and do not induce tissue remodeling if repeatedly administered. These studies provide an intriguing explanation for the increased incidence of symptoms in virus-infected smokers versus nonsmokers (22, 23), the enhanced severity of influenza in smokers versus nonsmokers (22, 24, 25), and the finding that virus-induced COPD exacerbations are more severe, last longer, and are associated with greater inflammatory responses and loss of lung function than exacerbations due to other causes (15, 19–21). Because these responses were seen in mice that were tran-

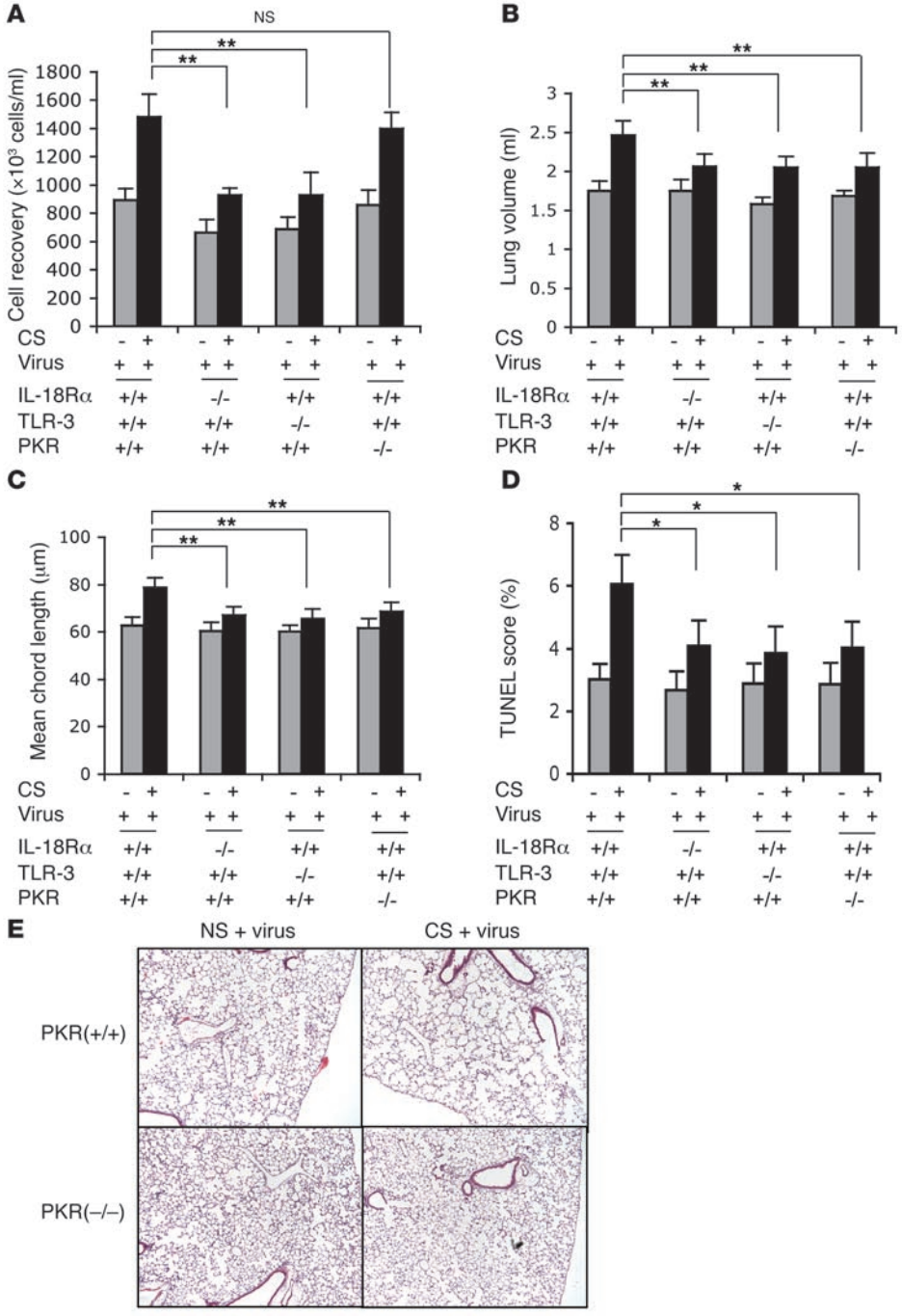

Figure 11
Roles of TLR3, IL-18Rα, and PKR in the inflammatory and remodeling effects of influenza virus and CS. Mice were exposed to CS or RA (CS–) for 2 weeks and then infected with influenza virus (virus+) or vehicle control (virus–). (**A**) Effects of this intervention on total BAL cell recovery 9 days after viral inoculation. Lung volume (**B**), mean chord length (**C**), TUNEL staining (**D**), and alveolar histology (**E**) were assessed 15 days after viral inoculation. Parts **A**–**D** represent the mean ± SEM of evaluations in a minimum of 5 mice. Part **E** is representative of 4 similar evaluations. Original magnification, ×4. *$P < 0.05$; **$P < 0.01$.

siently exposed to CS, these findings also have important implications in regard to the potential health consequences of secondhand smoke and the mechanisms that may mediate the effects of smoke in this setting.

Historically, bacteria have been considered to be the main infectious cause of COPD exacerbations (13). However, modern PCR-based diagnostic approaches have demonstrated that viruses are major contributors in 39% of outpatient exacerbations and a higher percentage of patients with severe exacerbations (13, 20, 21). Our demonstration that CS selectively augments viral PAMP–induced and live virus–induced inflammation and remodeling has a number of implications in regard to the pathogenesis and treatment of COPD. First, recent studies have demonstrated that RSV can be detected in the lower airway of patients with stable COPD and that these patients have higher levels of inflammation and an accelerated loss of lung function compared with RSV-negative individuals (20, 45). Since studies from our laboratory have demonstrated that CS synergizes with RSV in a manner that is analogous to influenza (C.S. Dela Cruz, M.-J. Kang, and J.A. Elias, unpublished observations), it is tempting to speculate that this CS-RSV interaction is responsible for the exaggerated responses in these patients. Our findings also

provide a strong rationale for thorough viral diagnostic evaluations in patients with COPD exacerbations and suggest that interventions that alter the activation of the MAVS, TLR3, IL-18, IL-18Rα, IL-12/IL-23 p40, IFN-γ, PKR, and eIF2α pathways that mediate these responses may have therapeutic utility.

Host antiviral responses are initiated via the detection of viral PAMPs by host pattern recognition receptors (PRRs) (35, 36). Upon recognition, PRR signaling results in the expression of type I IFNs that suppress viral replication and facilitate adaptive immune responses (35, 36). dsRNA, which is produced during the replication of many viruses, is recognized by several innate pathways including TLR3 and the RNA helicases RIG-1 and Mda5 (35, 36). In addition, many single-stranded RNA viruses, including influenza, have been shown to activate the RIG-1 pathway via the generation of 5′-triphosphorylated single-stranded RNA. TLR3 resides in endosomal membranes where it recognizes dsRNA and poly(I:C). RIG-1 and Mda5 detect dsRNA and poly(I:C) in the cytoplasm (35) where they are linked to downstream signaling molecules via MAVS (35, 36). When we started these studies, we hypothesized that the heightened inflammatory and remodeling responses induced by poly(I:C) in mice exposed to CS would be mediated to a great extent by TLR3. Our studies demonstrated that this is not entirely correct because the acute and chronic inflammatory and remodeling responses induced by CS plus poly(I:C) were mediated by partially TLR3-dependent and TLR3-independent pathways, respectively. In light of the limited roles of TLR3 in these responses, the contributions of the spiral helicase pathway were evaluated. These studies demonstrated that the synergistic interactions of poly(I:C) and CS were significantly ameliorated in the absence of MAVS. They also demonstrated that PKR and eIF2α were activated by CS plus poly(I:C) via a MAVS-dependent mechanism or mechanisms. These are the first studies, to our knowledge, to highlight the ability of CS to regulate the activation of this spiral helicase pathway. We believe they are also the first to demonstrate that this helicase pathway can regulate the activation of PKR and eIF2α. Additional investigation will be required to define the mechanisms of helicase-MAVS activation and MAVS-pathway regulation of PKR and eIF2α.

PKR is a serine threonine kinase (reviewed in ref. 41) that was initially discovered as an IFN-induced and -activated gene that mediated antiviral effects largely via its ability to activate eIF2α and inhibit protein translation. It is now known to be activated by viruses, dsRNA, cytokines, growth factors, oxidative stress, and ceramide. After activation, it plays an important role in cell signaling and regulates gene transcription, at least in part, via its ability to interact with known signaling pathways, including NF-κB, MAP kinases, p53, STATs, and IFN regulatory factor 1 (IRF1) (41). As a result, it is now appreciated that it also plays an important role in the regulation of cell proliferation and differentiation, tumor suppression, and cellular apoptosis (40–42). Our studies demonstrate that CS interacts with viral PAMPs and live virus to activate PKR and eIF2α and that this induction is mediated via a MAVS-, IL-18Rα–, and IFN-γ–dependent mechanism. Our studies also demonstrate that PKR plays an important role in the pathogenesis of the inflammatory, apoptotic, and emphysematous responses induced by viral PAMPs and live virus in CS-exposed mice. We believe these are the first studies to demonstrate that CS regulates the PKR pathway and the first studies to implicate PKR and eIF2α activation in the pathogenesis of the inflammation, apoptosis, or emphysema in COPD. When viewed in combination, our data suggest that PKR and eIF2α are activated by a MAVS/IL-18/IFN-γ cascade in mice exposed to CS and viral PAMPs or live virus and that PKR and eIF2α contribute to the pathogenesis of pulmonary emphysema at least in part via their ability to induce pulmonary structural cell apoptosis.

In summary, our studies demonstrate that CS selectively augments viral PAMP and live virus–induced airway and alveolar inflammation and remodeling in the murine lung and highlight TLR3-dependent and independent and MAVS/PKR/IL-18Rα/IFN-γ–dependent pathway or pathways that contribute to the pathogenesis of these responses. These studies provide insights into mechanisms that can contribute to the pathogenesis of virus-induced COPD exacerbations and lung function deterioration, the enhanced severity of viral infections in smokers, and the toxic effects of second-hand smoke. They also identify new targets against which therapies can be developed to modulate the severity of virus-induced responses in these clinical settings.

Methods

Reagents. We purchased poly(I:C) from Amersham Biosciences and LPS, CpG, GDQ, and IMQ from InvivoGen. For immunoblot analysis, antibodies against β-actin, caspase-3, PKR, PARP, eIF2α, and p-eIF2α were purchased from Cell Signaling Technology. p-PKR antibody was from Sigma-Aldrich. The antibodies against CCSP and CD31 were from Santa Cruz Biotechnology Inc., and the antibody against pro–SP-C was from Millipore. The IFN-α/β standard for the type I IFN bioassay was purchased from Access Biomedical Diagnostics.

Mice. C57BL/6J WT, *IL-18Rα*$^{-/-}$, and *IFN-γ*$^{-/-}$ mice (46, 47) were obtained from The Jackson Laboratory. *PKR*$^{-/-}$ mice were gifts from Bryan R.G. Williams (Cleveland Clinic Foundation, Cleveland, Ohio) (48). *TLR3*$^{-/-}$ mice were gifts from Richard A. Flavell (Yale University) (49). MAVS-null mice were generated by our laboratory as previously described (36). All animal studies were approved by the Yale Institutional Animal Care and Use Committee.

Cigarette smoking exposure. Ten-week-old C57BL/6J mice were exposed to RA or the smoke from nonfiltered research cigarettes (2R4; University of Kentucky, Lexington, Kentucky, USA) using the smoking apparatus described by Shapiro et al. (50). During the first week, mice received a half cigarette twice a day to allow for acclimation. During the remainder of the exposure, they received 3 cigarettes per day (1 cigarette/session, 3 sessions/d). In selected experiments, BALB/c mice were utilized in a similar fashion.

In vivo administration of PAMPs. After 2 weeks of CS exposure, the mice were anesthetized and 50 μl aliquots of various PAMPs [poly(I:C), LPS, CpG, GDQ, and IMQ] or their vehicle controls were administered twice per week (every Monday and Thursday) for 2 weeks (days 15, 18, 22, and 25, respectively) via nasal aspiration. CS exposure was continued during this interval. At the desired time point, the mice were sacrificed and evaluated. For the experiments, mice were sacrificed 1 day after each administration.

In vivo administration of influenza virus. After 2 weeks of CS exposure, the mice were lightly anesthetized and $5.0 \times 10^{3.375}$ $TCID_{50}$ (50% tissue culture infective doses) of A/PR8/34 influenza (equivalent to 0.05 LD_{50} in C57BL/6J mice) was administered via nasal aspiration in 50 μl of serum-free medium, using techniques previously described by our laboratories (51). The mice were then sacrificed at postinfection days 3, 6, 9, 12, and 15. The lungs that were to be used for assessments of viral titer were snap-frozen in liquid nitrogen.

Determination of whole-lung influenza titers. Lungs were thawed and then homogenized prior to plating serial 10-fold dilutions in triplicate and then adding Madin-Darby canine kidney cells to all wells in DMEM-5. The following day, 0.0002% trypsin (Sigma-Aldrich) was added. Four days later, chicken red blood cells were added to each well (50 μl of a 0.5% suspension),

and wells with evidence of hemagglutination after 4 hours were counted. $TCID_{50}$ was calculated according to the method of Reed and Muench, a simple method of estimating 50% endpoints (52).

BAL. Mice were sacrificed using intraperitoneal ketamine/xylazine injection, and the trachea was cannulated and perfused with two 0.9-ml aliquots of cold saline. The cellular contents and BAL fluid were separated by centrifugation, and the BAL fluid was stored in aliquots at –80°C.

Assessment of lung volume. Lungs were removed from control and test mice and inflated slowly at a constant pressure of 25 cm. Lung volume was then assessed by volume displacement using saline and a graduated cylinder as previously described by our laboratory (53, 54).

Lung morphometry. The right main bronchus was ligated, and the left lung was inflated with 0.5% low temperature–melting agarose in STRECK fixative at a constant pressure of 25 cm. This allowed for homogenous expansion of lung parenchyma as described by Halbower et al. (55). The lungs were then fixed, paraffin embedded, and H&E stained. Ten random fields were evaluated by microscopic projection onto the NIH Image program (ver. 1.63), and alveolar size was estimated from the mean chord length of the air space as described previously by our laboratory (34).

Quantification of BAL fluid cytokines. The levels of BAL IL-18 (MBL International Corp.), IL-12/IL-23 p40, and IFN-γ (R&D Systems) were determined using commercial ELISA kits as per the manufacturer's instructions.

IFN-α/β bioassay. Samples were acid treated to a pH of 2 to inactivate any input virus as well as other cytokines. The samples were then neutralized with sodium bicarbonate, and 2-fold dilutions of each test sample were added to murine fibroblast monolayers in 96-well plates. After overnight incubation at 37°C, 1.25×10^5 PFUs of vesicular stomatitis virus (VSV) were added to each well. An IFN-α/β standard was used in parallel to generate a standard curve. Additional controls included untreated monolayers with and without VSV infection. After 2 days of incubation, wells were fixed with 2% formaldehyde and stained with crystal violet. Test sample IFN-α/β concentrations were determined by comparison of protection from VSV-induced cell killing with that seen with known amounts of IFN-α/β.

IL-18 IHC. The localization of IL-18 was accomplished by IHC as described by our laboratory (34). In all cases, the specificity of the staining was evaluated by comparing the staining when the primary antibody was used and when it was excluded and by comparing the staining in WT and IL-18–null mice.

TUNEL analysis. End labeling of exposed 3′-OH ends of DNA fragments in paraffin-embedded tissue was undertaken with the TUNEL in situ cell death detection kit AP (Roche Diagnostics), using the instructions provided by the manufacturer. Staining specificity was assessed by comparing the signal that was seen when terminal transferase was included and excluded from the reaction. At least 10 random sections were obtained from each lung. After staining, a minimum of 300 cells were visually evaluated in each section. The labeled cells were expressed as a percentage of total nuclei.

Double-label IHC. Double-label IHC was undertaken using a modification of procedures described previously by our laboratory (34). TUNEL staining was undertaken as described above. IHC was then undertaken with antibodies against SP-C, CD31, or CCSP to identify type II alveolar epithelial cells, endothelial cells, and airway Clara cells, respectively. Anti-CCSP, anti-CD31, and anti–SP-C were used at 1:1000, 1:1000, and 1:500, respectively, and incubated overnight at 4°C. Images were photographed on an Olympus BH-2 fluorescent microscope.

Immunoblot analysis. Whole-lung lysates were prepared and the total protein content of each was measured using the DC protein assay reagents (Bio-Rad). Equal amounts of sample proteins were fractionated on 4%–15% SDS-PAGE gels under reducing conditions. These were individual gels that were prepared and run at the same time. The sample proteins were transferred to polyvinylidene difluoride membranes, then incubated in blocking buffer (5% w/v nonfat dry milk in TBS/0.05% Tween) for 1 hour at room temperature. They were then incubated with primary antibodies overnight at 4°C, washed 3 times in TBS/0.05% Tween, and incubated for 2 hours at room temperature with appropriate secondary antibodies. Immunoreactive signal was detected using a chemiluminescent procedure (ECL Western blotting detection system; Amersham) according to the manufacturer's instructions.

Statistics. Statistical evaluations were undertaken with SPSS software. As appropriate, groups were compared with 2-tailed Student's *t* test or with nonparametric Mann-Whitney *U* test. Values are expressed as mean ± SEM. Statistical significance was defined at a level of $P < 0.05$.

Acknowledgments

The authors thank Kathleen Bertier for excellent administrative assistance. These studies were funded by NIH grants HL-56389, HL-064242, HL-078744, HL-079328 (to J.A. Elias), and HL-084425 (to C.G. Lee).

Received for publication May 17, 2007, and accepted in revised form June 11, 2008.

Address correspondence to: Jack Elias, Department of Internal Medicine, Yale University School of Medicine, 333 Cedar Street (1072 LMP), PO Box 208056, New Haven, Connecticut 06520-8056, USA. Phone: (203) 785-4119; Fax: (203) 785-6954; E-mail: jack.elias@yale.edu.

1. Hogg, J.C., et al. 2004. The nature of small-airway obstruction in chronic obstructive pulmonary disease. *N. Engl. J. Med.* **350**:2645–2653.
2. Senior, R.M., and Shapiro, S.D. 1998. Chronic obstructive pulmonary disease: epidemiology, pathophysiology, and pathogenesis. In *Fishman's pulmonary diseases and disorders*. A.P. Fishman, et al., editors. McGraw-Hill. New York, New York, USA. 659–681.
3. Sutherland, E.R., and Cherniack, R.M. 2004. Management of chronic obstructive pulmonary disease. *N. Engl. J. Med.* **350**:2689–2697.
4. Hurst, J.R., Donaldson, G.C., Wilkinson, T.M., Perera, W.R., and Wedzicha, J.A. 2004. Relationships between the common cold and exacerbation frequency in COPD. *Eur. Respir. J.* **24**(Suppl. 48):686s.
5. Saetta, M., et al. 1999. CD8+ve cells in the lungs of smokers with chronic obstructive pulmonary disease. *Am. J. Respir. Crit. Care Med.* **160**:711–717.
6. Saetta, M., et al. 1994. Airway eosinophilia in chronic bronchitis during exacerbations. *Am. J. Respir. Crit. Care Med.* **150**:1646–1652.
7. Segura-Valdez, L., et al. 2000. Upregulation of gelatinases A and B, collagenases 1 and 2, and increased parenchymal cell death in COPD. *Chest.* **117**:684–694.
8. Yokohori, N., Aoshiba, K., and Nagai, A. 2004. Increased levels of cell death and proliferation in alveolar wall cells in patients with pulmonary emphysema. *Chest.* **125**:626–632.
9. Donaldson, G.C., et al. 2005. Airway and systemic inflammation and decline in lung function in patients with COPD. *Chest.* **128**:1995–2004.
10. Sapey, E., and Stockley, R.A. 2006. COPD exacerbations. 2: aetiology. *Thorax.* **61**:250–258.
11. Donaldson, G.C., Seemungal, T.A., Bhowmik, A., and Wedzicha, J.A. 2000. The relationship between exacerbation frequency and lung function decline in chronic obstructive pulmonary disease. *Thorax.* **57**:847–852.
12. Mallia, P., et al. 2007. Exacerbations of asthma and chronic obstructive pulmonary disease (COPD): focus on virus induced exacerbations. *Curr. Pharm. Des.* **13**:73–97.
13. Mallia, P., and Johnston, S.L. 2006. How viral infections cause exacerbation of airway diseases. *Chest.* **130**:1203–1210.
14. Kanner, R.E., Anthonisen, N.R., and Connett, J.E. 2001. Lower respiratory illnesses promote FEV(1) decline in current smokers but not ex-smokers with mild chronic obstructive pulmonary disease: results from the lung health study. *Am. J. Respir. Crit. Care Med.* **164**:358–364.
15. Wedzicha, J.A. 2004. Role of viruses in exacerbations of chronic obstructive pulmonary disease. *Proc. Am. Thorac. Soc.* **1**:115–120.
16. Ko, F.W., et al. 2007. A 1-year prospective study of the infectious etiology in patients hospitalized with acute exacerbations of COPD. *Chest.* **131**:44–52.
17. O'Gorman, C., McHenry, E., and Coyle, P.V. 2006. Human metapneumovirus in adults: a short case series. *Eur. J. Clin. Microbiol. Infect. Dis.* **25**:190–192.
18. Sajjan, U.S., et al. 2006. H. influenzae potentiates airway epithelial cell responses to rhinovirus by increasing ICAM-1 and TLR3 expression. *FASEB J.* **20**:2121–2123.
19. Bhowmik, A., Seemungal, T.A., Sapsford, R.J., and

Wedzicha, J.A. 2000. Relation of sputum inflammatory markers to symptoms and lung function changes in COPD exacerbations. *Thorax.* **55**:114–120.
20. Seemungal, T., et al. 2001. Respiratory viruses, symptoms, and inflammatory markers in acute exacerbations and stable chronic obstructive pulmonary disease. *Am. J. Respir. Crit. Care Med.* **164**:1618–1623.
21. Tan, W.C., et al. 2003. Epidemiology of respiratory viruses in patients hospitalized with near-fatal asthma, acute exacerbations of asthma, or chronic obstructive pulmonary disease. *Am. J. Med.* **115**:272–277.
22. Arcavi, L., and Benowitz, N.L. 2004. Cigarette smoking and infection. *Arch. Intern. Med.* **164**:2206–2216.
23. Cohen, S., Tyrrell, D.A., Russell, M.A., Jarvis, M.J., and Smith, A.P. 1993. Smoking, alcohol consumption, and susceptibility to the common cold. *Am. J. Public Health.* **83**:1277–1283.
24. Kark, J.D., and Lebiush, M. 1981. Smoking and epidemic influenza-like illness in female military recruits: a brief survey. *Am. J. Public Health.* **71**:530–532.
25. Kark, J.D., Lebiush, M., and Rannon, L. 1982. Cigarette smoking as a risk factor for epidemic a(h1n1) influenza in young men. *N. Engl. J. Med.* **307**:1042–1046.
26. Papi, A., et al. 2006. Infections and airway inflammation in chronic obstructive pulmonary disease severe exacerbations. *Am. J. Respir. Crit. Care Med.* **173**:1114–1121.
27. Barr, J., et al. 2007. Nicotine induces oxidative stress and activates nuclear transcription factor kappa B in rat mesencephalic cells. *Mol. Cell. Biochem.* **297**:93–99.
28. Sopori, M. 2002. Effects of cigarette smoke on the immune system. *Nat. Rev. Immunol.* **2**:372–377.
29. D'Hulst, A.I., et al. 2005. Cigarette smoke-induced pulmonary emphysema in scid-mice. Is the acquired immune system required? *Respir. Res.* **6**:147.
30. Gebel, S., et al. 2006. The kinetics of transcriptomic changes induced by cigarette smoke in rat lungs reveals a specific program of defense, inflammation, and circadian clock gene expression. *Toxicol. Sci.* **93**:422–431.
31. Hodge, S., Hodge, G., Scicchitano, R., Reynolds, P.N., and Holmes, M. 2003. Alveolar macrophages from subjects with chronic obstructive pulmonary disease are deficient in their ability to phagocytose apoptotic airway epithelial cells. *Immunol. Cell Biol.* **81**:289–296.
32. Vlahos, R., Bozinovski, S., Hamilton, J.A., and Anderson, G.P. 2006. Therapeutic potential of treating chronic obstructive pulmonary disease (COPD) by neutralising granulocyte macrophage-colony stimulating factor (GM-CSF). *Pharmacol. Ther.* **112**:106–115.
33. Schleimer, R.P. 2005. Innate immune responses and chronic obstructive pulmonary disease: "Terminator" or "Terminator 2"? *Proc. Am. Thorac. Soc.* **2**:342–346 discussion 371–342.;
34. Kang, M.J., et al. 2007. IL-18 is induced and IL-18 receptor alpha plays a critical role in the pathogenesis of cigarette smoke-induced pulmonary emphysema and inflammation. *J. Immunol.* **178**:1948–1959.
35. Kumar, H., et al. 2006. Essential role of IPS-1 in innate immune responses against RNA viruses. *J. Exp. Med.* **203**:1795–1803.
36. Sun, Q., et al. 2006. The specific and essential role of MAVS in antiviral innate immune responses. *Immunity.* **24**:633–642.
37. Kasahara, Y., et al. 2000. Inhibition of VEGF receptors causes lung cell apoptosis and emphysema. *J. Clin. Invest.* **106**:1311–1319.
38. Aoshiba, K., Yokohori, N., and Nagai, A. 2003. Alveolar wall apoptosis causes lung destruction and emphysematous changes. *Am. J. Respir. Cell Mol. Biol.* **28**:555–562.
39. Petrache, I., et al. 2005. Ceramide upregulation causes pulmonary cell apoptosis and emphysema-like disease in mice. *Nat. Med.* **11**:491–498.
40. Der, S.D., Yang, Y.L., Weissmann, C., and Williams, B.R. 1997. A double-stranded RNA-activated protein kinase-dependent pathway mediating stress-induced apoptosis. *Proc. Natl. Acad. Sci. U. S. A.* **94**:3279–3283.
41. Garcia, M.A., et al. 2006. Impact of protein kinase PKR in cell biology: from antiviral to antiproliferative action. *Microbiol. Mol. Biol. Rev.* **70**:1032–1060.
42. Guerra, S., Lopez-Fernandez, L.A., Garcia, M.A., Zaballos, A., and Esteban, M. 2006. Human gene profiling in response to the active protein kinase, interferon-induced serine/threonine protein kinase (PKR), in infected cells. Involvement of the transcription factor ATF-3 IN PKR-induced apoptosis. *J. Biol. Chem.* **281**:18734–18745.
43. Hsu, L.C., et al. 2004. The protein kinase PKR is required for macrophage apoptosis after activation of Toll-like receptor 4. *Nature.* **428**:341–345.
44. Robbins, C.S., et al. 2006. Cigarette smoke impacts immune inflammatory responses to influenza in mice. *Am. J. Respir. Crit. Care Med.* **174**:1342–1351.
45. Wilkinson, T.M., Donaldson, G.C., Johnston, S.L., Openshaw, P.J., and Wedzicha, J.A. 2006. Respiratory syncytial virus, airway inflammation, and FEV1 decline in patients with chronic obstructive pulmonary disease. *Am. J. Respir. Crit. Care Med.* **173**:871–876.
46. Dalton, D.K., et al. 1993. Multiple defects of immune cell function in mice with disrupted interferon-gamma genes. *Science.* **259**:1739–1742.
47. Hoshino, K., et al. 1999. Cutting edge: generation of IL-18 receptor-deficient mice: evidence for IL-1 receptor-related protein as an essential IL-18 binding receptor. *J. Immunol.* **162**:5041–5044.
48. Yang, Y.L., et al. 1995. Deficient signaling in mice devoid of double-stranded RNA-dependent protein kinase. *EMBO J.* **14**:6095–6106.
49. Alexopoulou, L., Holt, A.C., Medzhitov, R., and Flavell, R.A. 2001. Recognition of double-stranded RNA and activation of NF-kappaB by Toll-like receptor 3. *Nature.* **413**:732–738.
50. Hautamaki, R.D., Kobayashi, D.K., Senior, R.M., and Shapiro, S.D. 1997. Requirement for macrophage elastase for cigarette smoke-induced emphysema in mice. *Science.* **277**:2002–2004.
51. Liu, J., et al. 2005. Requirement for tumor necrosis factor-receptor 2 in alveolar chemokine expression depends upon the form of the ligand. *Am. J. Respir. Cell Mol. Biol.* **33**:463–469.
52. Reed, L.J., and Muench, H. 1938. A simple method of estimating 50% endpoints. *Am. J. Hyg.* **27**:493–497.
53. Zheng, T., et al. 2005. Role of cathepsin S-dependent epithelial cell apoptosis in IFN-gamma-induced alveolar remodeling and pulmonary emphysema. *J. Immunol.* **174**:8106–8115.
54. Zheng, T., et al. 2000. Inducible targeting of IL-13 to the adult lung causes matrix metalloproteinase- and cathepsin-dependent emphysema. *J. Clin. Invest.* **106**:1081–1093.
55. Halbower, A.C., Mason, R.J., Abman, S.H., and Tuder, R.M. 1994. Agarose infiltration improves morphology of cryostat sections of lung. *Lab. Invest.* **71**:149–153.